frontiers in Energy Research

ORIGINAL RESEARCH
published: 09 April 2021
doi: 10.3389/fenrg.2021.653527

Identification of Active Surface Species in Molten Carbonates Using *in situ* Raman Spectroscopy

*Peng Zhang, Tao Wu and Kevin Huang**

Department of Mechanical Engineering, University of South Carolina, Columbia, SC, United States

Here we report the results of a study on active surface species of a pristine and modified $(Li\text{-}Na)_2CO_3$ eutectic using *in situ* Raman spectroscopy technique. The effects of gas compositions, temperature, time, and alkaline earth have been systematically studied. The species of CO_4^{2-}, HCO_4^-, and $C_2O_5^{2-}$ are identified as the three major active species on the surface of $(Li\text{-}Na)_2CO_3$ eutectic by a combined Raman spectroscopy and theoretical density functional theory calculations. The results further reveal that CO_4^{2-}, HCO_4^-, and $C_2O_5^{2-}$ are preferably formed in the presence of O_2, H_2O, and high CO_2 concentration. With the addition of Ba to the pristine $(Li\text{-}Na)_2CO_3$ eutectic, the Raman CO_4^{2-}/HCO_4^- shifts become more pronounced.

Keywords: molten carbonate, surface species, Raman spectroscopy, DFT, alkaline earth

OPEN ACCESS

Edited by:
Hossein Ghezel-Ayagh,
FuelCell Energy, United States

Reviewed by:
Chao-Yi Yuh,
FuelCell Energy, United States
Michel Cassir,
ParisTech École Nationale Supérieure de Chimie de Paris, France

***Correspondence:**
Kevin Huang
huang46@cec.sc.edu

Specialty section:
This article was submitted to Hydrogen Storage and Production, a section of the journal Frontiers in Energy Research

Received: *14 January 2021*
Accepted: *19 March 2021*
Published: *09 April 2021*

Citation:
Zhang P, Wu T and Huang K (2021) Identification of Active Surface Species in Molten Carbonates Using in situ Raman Spectroscopy. Front. Energy Res. 9:653527. doi: 10.3389/fenrg.2021.653527

INTRODUCTION

Molten carbonate fuel cells (MCFCs) are a class of energy-efficient and low-emission power generators (Morita et al., 2002; Watanabe et al., 2006; Kawase, 2017). One of their unique features is the use of CO_2 and O_2 as the cathode gas. The mixture of CO_2 and O_2 is also a major component in flue gas produced by either coal-fired or natural-gas (NG)-fired power plants. A natural and logical question is if the flue gas can be directly utilized as the oxidant by MCFCs to produce additional power while mitigating the CO_2 emission.

The concentration of CO_2 emitted by coal-fired power plants is more than twice that emitted by NG-fired power plants, e.g., 10 vs. 4%. The current benchmark MCFCs can operate normally with a CO_2 concentration higher than 10%; at lower CO_2 concentrations, their performance is significantly limited by diffusion-related concentration polarization. To generate power from MCFCs using low CO_2 concentration flue gas produced from NG-fired power plants, the existing MCFC cell/stack technology needs to be further improved to minimize the concentration polarization and meet the performance requirements. In addition, there is a significant amount of H_2O, e.g., 10%, in NG flue gas. The effect of H_2O on the MCFC performance is not well understood from early studies.

A recent result has confirmed that MCFCs exhibit a high concentration-polarization at low CO_2 concentrations and surprisingly enhanced performance in the presence of H_2O (Rosen et al., 2020). An electrochemical model based on active species peroxide-ion (O_2^{2-}) and superoxide (O_2^-) has been proposed with satisfactory agreement with the experimental data (Cassir et al., 1993). Indeed, an independent Raman spectroscopy study has confirmed the existence of O_2^{2-} on the surface of a Li_2/K_2CO_3 eutectic (Chen et al., 2004).

A parallel conduction mechanism is also proposed for OH^- as a working ion when H_2O is present in the oxidant feed. From the water mass collected at both cathode and anode sides, it appears to suggest that the conduction mechanism of OH^- in a MC matrix is real (Rosen et al., 2020). However, more experimental evidence related to active species to support water transport is needed.

Raman spectroscopy is a very sensitive technique to detect vibrational modes of C-O-C, C-O, and C = O bonds that are abundant in C-containing species such as CO_3^{2-} and CO_4^{2-} and are of interest to this research (Itoh et al., 2004; Mendoza et al., 2004). We have previously used Raman spectroscopy to probe the surface chemistry of an Ag-MC (Molten Carbonate) membrane operated under a flue gas condition containing O_2 and CO_2 to facilitate our understanding of why enhanced oxygen permeation was observed (Tong et al., 2016). We concluded from both experimental and theoretical data that $LiCO_4^-$ was the active species on the Ag-MC membrane surface under simulated flue gas conditions and the extra oxygen in CO_4^{2-} ligand relative to CO_3^{2-} is the reason for the increased oxygen transport. The *in situ* Raman spectra of the Ag-MC membrane were collected by a LabRam/HR confocal Raman system (LabRam Invers, Horiba Jobin-Yvon) equipped with a 632.8 nm He-Ne laser and hot stage (Linkam TS1500, 0–1,500°C). From this work, we were able to identify that CO_4^{2-} is an active species on the surface of an atomic layer deposition Al_2O_3-coated Ag-MC composite membrane and explain the phenomenon of the enhanced oxygen flux based on the percarbonate mechanism. In a similar work (Mendoza et al., 2004), we were also able to identify the active surface species as $C_2O_5^{2-}$ with *in situ* Raman spectroscopy when a MC melt was exposed to a pure CO_2 atmosphere.

These prior works demonstrate the versatility and capability of *in situ* Raman spectroscopy in probing active species on the surface of MC. Therefore, in this study, the *in situ* Raman spectroscopy technology was selected to identify the species of molten carbonate exposed to varies atmospheres at MCFC operating temperatures.

EXPERIMENTAL

Sample Preparation

The molten carbonate compositions under this study were Li_2CO_3-Na_2CO_3 eutectic with a ratio of 52:48 mol% (MC), and 10 mol%-$SrCO_3$ added MC (Sr-MC) and 10 mol%-$BaCO_3$ added MC (Ba-MC). The reason for selecting Li_2CO_3-Na_2CO_3 eutectic was primarily based on the consideration of its higher ionic conductivity than other alkali carbonates eutectics. To prevent MC overflow at high temperatures, an Ag porous matrix was used to contain all MCs. The Ag porous matrix was prepared in the same way as in our previous study (Zhang et al., 2016). Briefly, Ag powders (99.9% metal basis, Alfa Aesar) were mixed with carbon black as a pore former in a volume ratio of 1:1 in ethanol. The dried power mixture was then pressed into pellets under 70 MPa, followed by sintering at 650°C for 2 h in air to remove the carbon pore former and achieve good mechanical strength. Then the porous Ag pellet was soaked into a MC at 650°C for 2 h in air, forming Ag/MC composite.

Characterization

The Raman system used for this study is a Horiba Jobin-Yvon LabRAM HR800. It features a focal length of 800 mm, spectral length of 100–4,000 cm^{-1} with a spectral resolution up to 1.5 cm^{-1}, accuracy of wavenumber of 1 cm^{-1} and spatial resolution up to 1 μm. We use the following operating parameters for Raman spectroscopy study on the surface of a MC:

- Wavelength: 300–1,800 cm^{-1}
- Light source: 632 nm red
- Acquisition time: 20 s
- Accumulation: 1
- Hole: 500
- Filter: 100%.

The system is also adaptable to high-temperature subsystem for *in situ* measurements. The high temperature unit (or herein called hot stage) is model Linkam TS1500. The hot-stage is connected to a water-cooling system driven by a water circulation pump. The actual temperature was calibrated with the melting point of prepared MC (490°C), and temperature effect was studied at 575 and 625°C. Since the atmosphere effect is a focus of the study, we systematically varied the gas compositions over the MC at a temperature. **Table 1** lists all the gas mixtures studied. The total gas flow was fixed at 50 sccm for all measurements.

DFT Calculations

The equilibrium geometries of species were fully optimized at the B3LYP/6-311G* level using the Gaussian 09 program package (Hehre, 2002; Frisch et al., 2009). To better understand the vibrational modes and figure out fingerprints of these species, Raman spectra were simulated using the B3LYP/6-311G* basis sets under the harmonic approximation at the same level of geometry optimization. Vibrational analysis showed that all the structures were at minima in the potential energy surface (no imaginary frequencies). Based on the Raman activity obtained from density functional theory (DFT) calculations, the Raman intensity was determined by the GaussSum software (O'Boyle et al., 2008).

TABLE 1 | Gas compositions tested under this project.

Run	O_2 (%)	CO_2 (%)	H_2O (%)	N_2 (%)
#1	0	0	0	100
#2	10	2	0	Bal.
#3	10	10	0	Bal.
#4	9	2	10	Bal.
#5	9	9	10	Bal.
#6	9	45	10	Bal.
#7	0	90	10	0

RESULTS AND DISCUSSION

Comparison of Raman Spectra in Dry Gas

Figure 1 compares the Raman spectra at 575°C in pure N_2 (gas #1), 2% CO_2 (gas #2), and 10% CO_2 (gas #3) atmospheres. The lower intensity of the Raman spectra in 10% CO_2 is due to the presence of Ag in the Ag-MC sample used to prevent the overflow of the MC. In the following studies, all Raman spectra were collected with the Ag-MC sample. As shown in the **Figure 1**, the main band at 1,072 cm^{-1} is assigned to symmetric stretching (v_1) of O-C-O, where the bands at 707, 885, 1,391, 1,500, and 1,762 cm^{-1} correspond to the in-plane bending (v_4) of C-O, out-of-plane bending (v_2) of O-C-O, doubly degenerate asymmetric stretching (v_3) of O-C-O, and the overtone of the out-of-plane bending mode ($2v_2$) vibrations, respectively (Bates et al., 1972; Chen et al., 2002; Zhang et al., 2013). Clearly, there is no difference in these Raman shifts, implying that dry N_2 and CO_2 conditions do not invoke new species other than CO_3^{2-}. Similar phenomenon was also observed in our previous study, where there is no new peak in the dry gas conditions with Ag-MC sample (Tong et al., 2016).

The temperature and time effect on the Raman spectra of the Ag-MC samples in dry 10% CO_2 atmosphere (gas #3) are compared in **Figure 2**. **Figures 2A,B** show the Raman spectra of the Ag-MC sample at 575 and 625°C, respectively. These results confirm that there is no difference in spectrum in dry gas at both temperatures.

CO_2 Concentration Effect in Wet Gas

To investigate why steam promotes the MCFC performance, we also conducted the Raman spectroscopy of the Ag-MC sample in wet gas (10% H_2O) with different CO_2 concentrations. For an easy comparison, the Raman spectra in dry N_2 is also shown in **Figure 3**. Some new shift between 400 and 607 cm^{-1} appear in wet CO_2 atmospheres. To identify these new shifts, DFT calculations were performed. From the DFT calculations, the weak but new shifts at 409 and 567 cm^{-1} seem to relate to HCO_4^-, while the weak but new shifts at 607 cm^{-1} can be assigned to CO_4^{2-}. These two species are observed in CO_2 concentration gases from 2 to 45% CO_2, while at high CO_2-concentraiton, e.g., 90% CO_2, $C_2O_5^{2-}$ species appears at 455 cm^{-1}. The observation of $C_2O_5^{2-}$ species at high CO_2 concentration is reasonable given the fact that CO_2 dissolution into MC to form $C_2O_5^{2-}$ by $CO_2+CO_3^{2-}=C_2O_5^{2-}$ (Claes et al., 1996).

When the gas atmosphere changed from dry N_2 to wet 2% CO_2, the weak but new bands at 567 and 607 cm^{-1} seem to emerge, which correspond to HCO_4^- and CO_4^{2-}, respectively. (Note: the wet 2% CO_2 gas also contains 9% O_2, see **Table 1**, gas #4). Then the intensity of the new bands slightly increased by increasing CO_2 concentration to 9 and 45%. The formation mechanisms for the observed HCO_4^- and CO_4^{2-} are (Zhang et al., 2014; Tong et al., 2016):

$$H_2O + 2CO_2 + 3/2O_2 + 2e^- = 2HCO_4^- \quad (1)$$

$$CO_2 + 3/2O_2 + CO_3^{2-} + 2e^- = 2CO_4^{2-} \quad (2)$$

From these reactions, H_2O is essential to form HCO_4^-, but not for CO_4^{2-} species. However, it is interesting to see that CO_4^{2-} appears in wet flue gas but not in dry flue gas (i.e., ~10% CO_2-10% O_2), see **Figure 2B**. A possible reason is that the steam facilitates the dissolution of O_2 into MC. From **Figure 3**, HCO_4^- and CO_4^{2-} bands disappear and $C_2O_5^{2-}$ band appear with

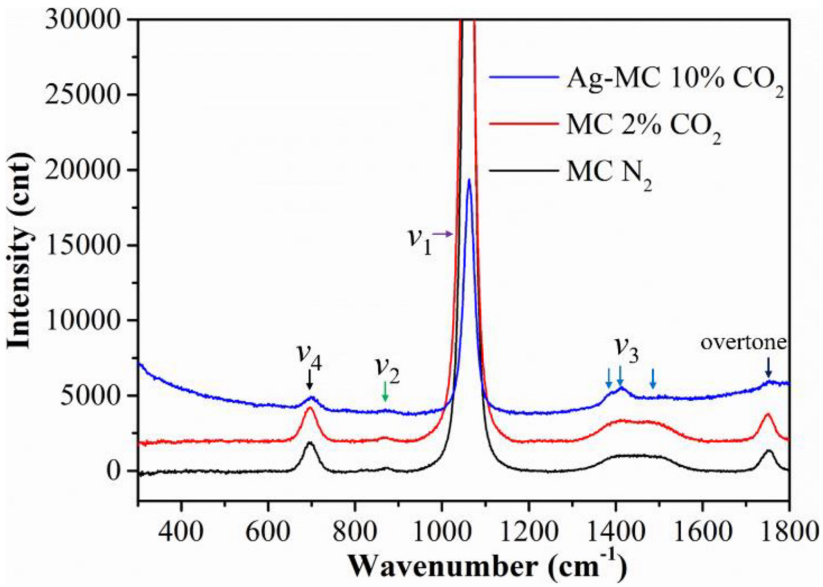

FIGURE 1 | The Raman spectra of the MC/Ag-MC samples at 575°C in dry gas atmospheres with different CO_2 concentration. (N_2: gas #1, 2% CO_2: gas #2, 10% CO_2: gas #3).

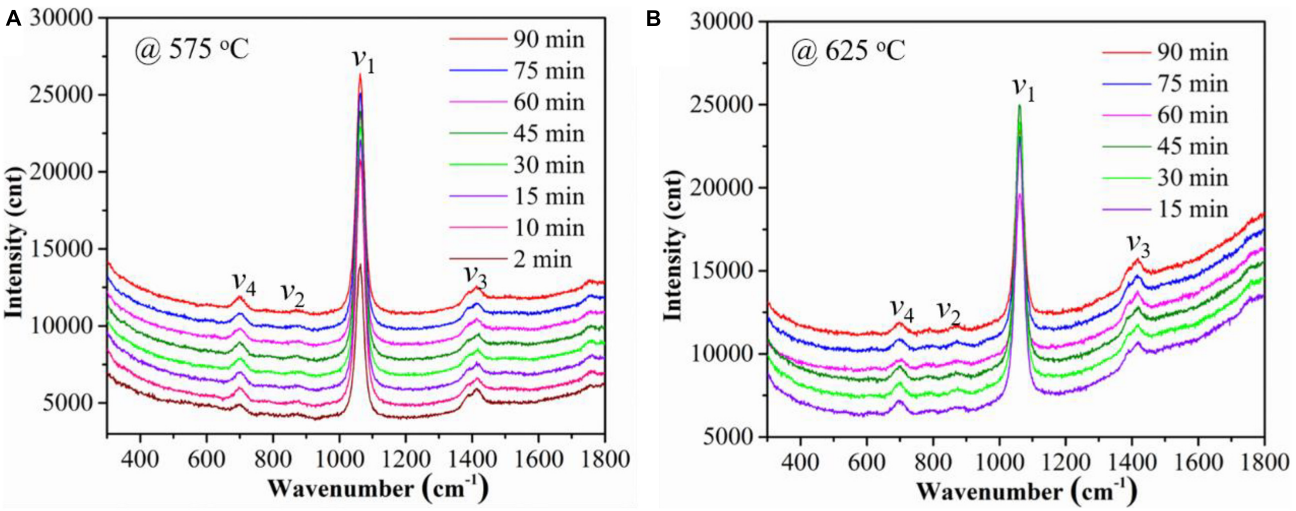

FIGURE 2 | The effects of temperature and time on Raman spectra of the Ag-MC sample in dry 10% CO_2 gas (gas #3). **(A)** 575°C and **(B)** 625°C.

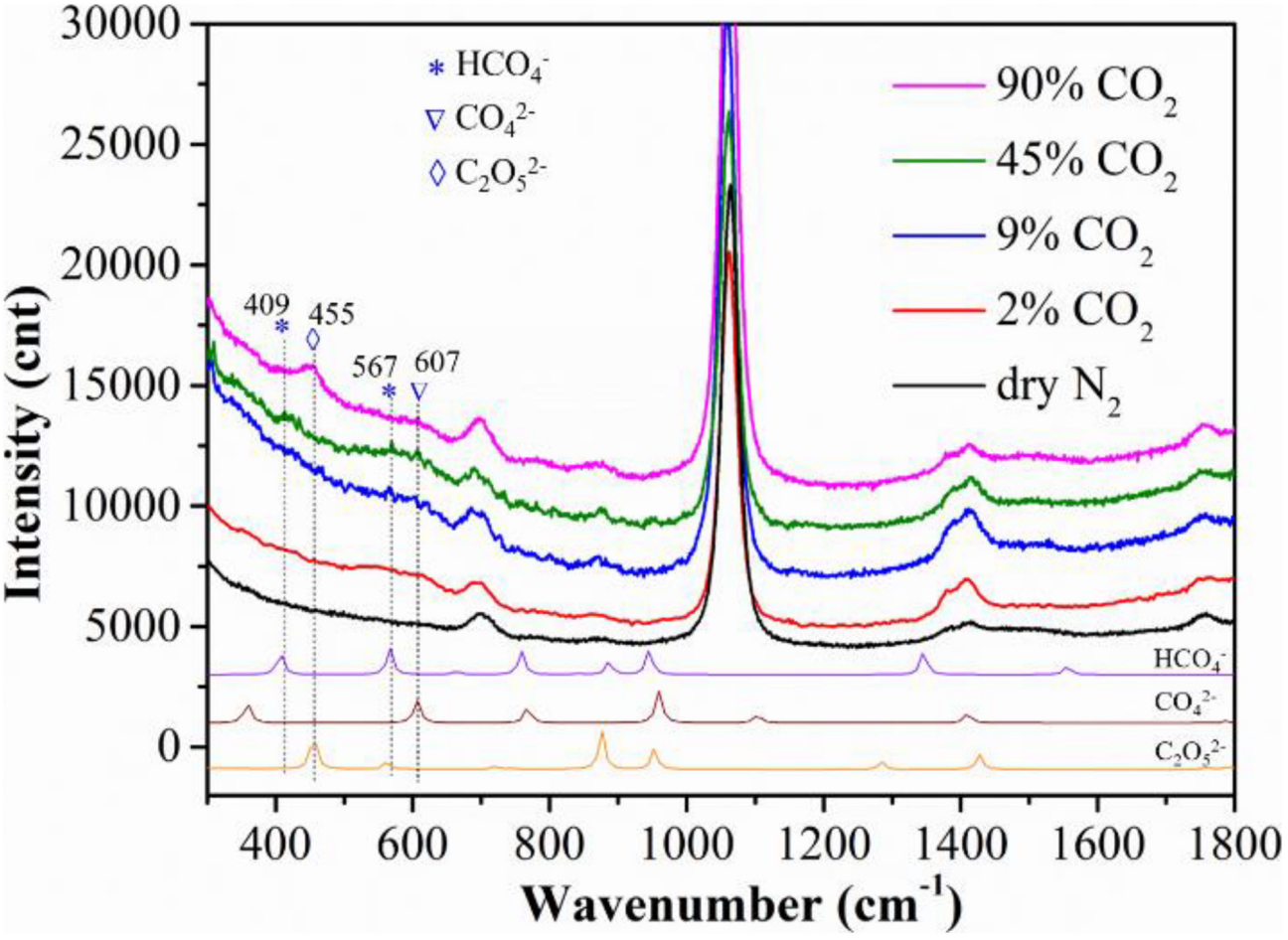

FIGURE 3 | Raman spectra, along with DFT calculations, of the Ag-MC sample collected at 625°C in different CO_2 concentration gas conditions: dry N_2 (gas #1), 2% CO_2 (gas #4), 9% CO_2 (gas #5), 45% CO_2 (gas #6), 90% CO_2 (gas #7).

further increasing CO_2 concentration to 90% (no O_2), which is consistent with our previous study (Zhang et al., 2013).

The Effect of Alkaline Earth-Addition to MC

To further confirm that the formation of HCO_4^- and CO_4^{2-} is highly influenced by the solubility of molecular oxygen, and therefore, the basicity in MCs. We measured the Raman spectra of alkaline earth-addition MC, since it has been reported that the alkaline earth metals can enhance the oxygen solubility of the molten carbonate (Scaccia and Frangini, 2009). At first, the Raman spectra of Ba- and Sr-added MC under in 45% CO_2-10% O_2-10% H_2O-N_2 atmosphere (gas #6) were collected and are shown in **Figure 4**. It seems that Sr-doped MC sample show similar new bands with the pristine MC sample. However, the intensities of HCO_4^- and CO_4^{2-} bands of Ba-added MC samples are increased appreciably. In addition, a couple of more pronounced new peaks at ~360 and 770 cm^{-1} are observed of the Ba-added sample. Compared to DFT-calculated Raman bands, it is determined that the new shift is related to CO_4^{2-}. These results further suggest that high oxygen solubility promotes the formation of CO_4^-.

Since both the H_2O and alkaline earth metals increase the oxygen solubility of MCs, we also conducted Raman study of the Ba-MC sample under dry gas condition. **Figure 5** shows that the Ba-MC sample does exhibit new surface species under CO_2-free, H_2O-free and wet gas conditions. Similar Raman spectra were obtained under the dry flue gas and wet 45% CO_2 atmosphere, confirming that the oxygen solubility highly influences the formation of CO_4^{2-} and HCO_4^-. **Figure 5** also shows significant appearance of new shifts at 403 and 803 cm^{-1} under dry 10% O_2 condition. DFT calculations suggest that it is related to $BaCO_3$. This finding implies that Ba-MC is unstable under dry 10% O_2-N_2, precipitating out $BaCO_3$ on the MC surface. However, in the presence of both H_2O and CO_2, $BaCO_3$ re-dissolves back into MC, but with a pronounced shift at ~600 cm^{-1} relating to species HCO_4^- and CO_4^{2-}. In addition, the new shift at 360 cm^{-1} is attributed to CO_4^{2-} according to the DFT calculation, further indicating that the Ba-added MC enhances oxygen solubility. For convenience, we show in **Figure 6** a schematic of the $BaCO_3$ precipitation and re-dissolution mechanisms in dry O_2 and CO_2-H_2O-O_2-containing gas mixtures, respectively.

Overall, based on the above Raman spectroscopic results, we propose the following mechanisms for CO_2 and H_2O transport in MCFCs with a high-basicity MC as the electrolyte, H_2 as the anode gas and $CO_2/H_2O/O_2$ as the cathode gas:

At Cathode:

$$\text{Main reaction}: \ CO_2 + 1/2O_2 + 2e^- = CO_3^{2-} \quad (3)$$

Parallel reaction (1) :

$$H_2O + 2CO_2 + 3/2O_2 + 2e^- = 2HCO_4^- (\text{intermediate}) \quad (4)$$

$$HCO_4^- + 2e^- = OH^- + CO_3^{2-} \quad (5)$$

At Anode:

$$\text{Main reaction}: \ CO_3^{2-} + H_2 = H_2O + CO_2 + 2e^- \quad (6)$$

$$\text{Parallel reaction (1)}: \ 2OH^- + H_2 = 2H_2O + 2e^- \quad (7)$$

Since HCO_4^- is virtually an intermediary species, the experimentally observed H_2O and CO_2 transport in MCFC are carried out by OH^- and CO_3^{2-}.

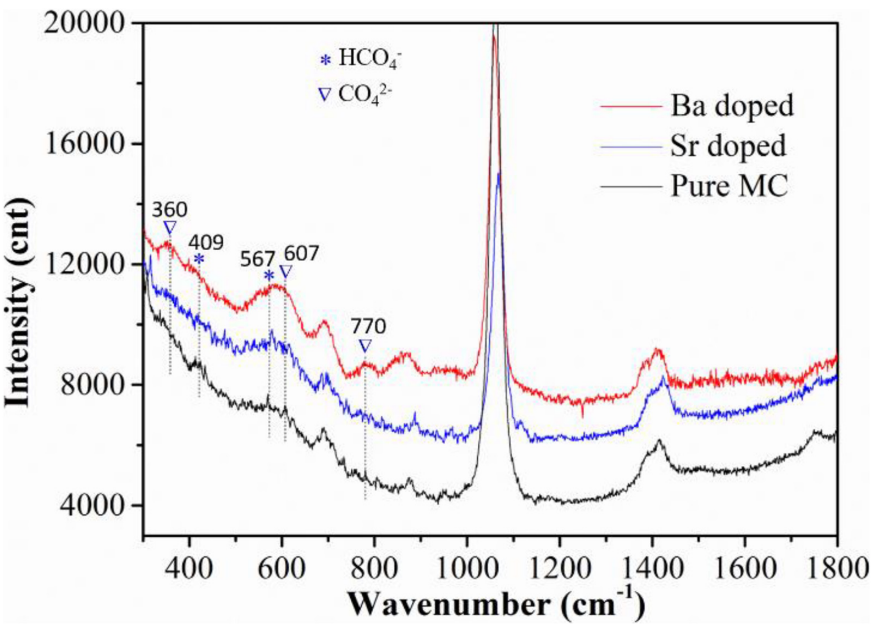

FIGURE 4 | Comparison of Raman spectra of three types of Li-Na MC (Ba-MC, Sr-MC, and MC) exposed to 45% CO_2-10% O_2-10% H_2O-N_2 atmosphere at 625°C.

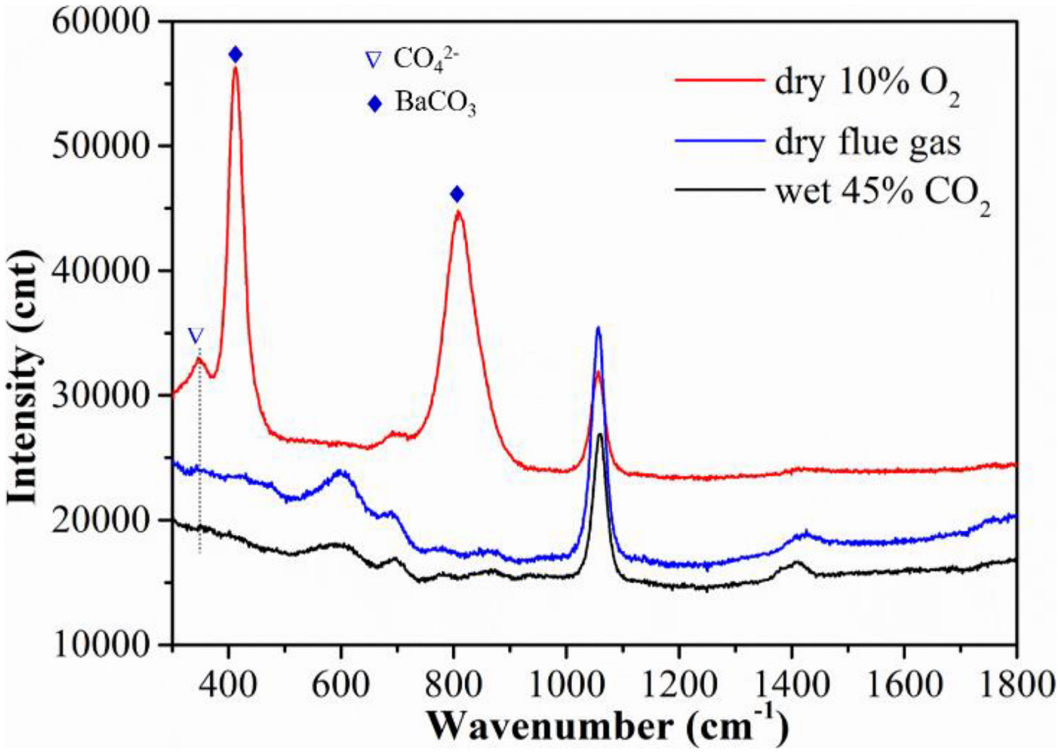

FIGURE 5 | Raman spectra of Ba-added MC collected under different gas conditions at 625°C.

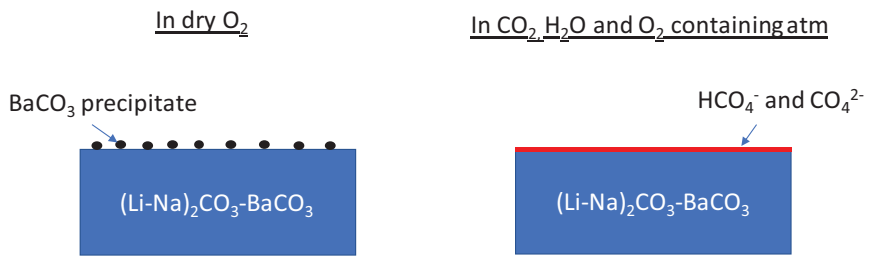

FIGURE 6 | Surface species of Ba-added MC exposed to different gas mixtures.

CONCLUSION

In summary, the surface chemistry of pristine and Ba- or Sr-modified Li-Na eutectic under seven gas mixtures has been studied by *in situ* Raman spectroscopy. Compared to the pristine MC under dry N_2, all the CO_2-containing dry gas conditions do not change Raman spectra of the MC. Under wet gas conditions, relatively weak new shifts appear in 300–700 cm^{-1} and their intensities increase with CO_2 concentration. Assisted by DFT calculations, the new shifts are identified to be CO_4^{2-}/HCO_4^- at low CO_2 concentrations and $C_2O_5^{2-}$ at high CO_2 concentrations. With the addition of Ba to the pristine MC, the CO_4^{2-}/HCO_4^- shifts become more pronounced due to enhanced oxygen solubility in MC. It was also discovered that $BaCO_3$ can precipitate out under CO_2-free dry gas environment. Based on the found surface intermediate species, a mechanism concerning H_2O and CO_2 co-transport is proposed.

DATA AVAILABILITY STATEMENT

The original contributions presented in the study are included in the article/supplementary material, further inquiries can be directed to the corresponding author/s.

AUTHOR CONTRIBUTIONS

PZ conducted the experiment. TW performed the DFT calculations. KH conceived the idea. All authors contributed to the article and approved the submitted version.

FUNDING

Financial supports from National Science Foundation (Award # 1924095) and ExxonMobil are greatly appreciated.

ACKNOWLEDGMENTS

The authors would like to acknowledge constructive discussion with Timothy A. Barckholtz, Gabor Kiss, and David Perkins at ExxonMobil.

REFERENCES

Bates, J. B., Brooker, M. H., Quist, A. S., and Boyd, G. E. (1972). Raman spectra of molten alkali metal carbonates. *J. Phys. Chem.* 76, 1565–1571. doi: 10.1021/j100655a013

Cassir, M., Moutiers, G., and Devynck, J. (1993). Stability and characterization of oxygen species in alkali molten carbonate: a thermodynamic and electrochemical approach. *J. Electrochem. Soc.* 140:3114. doi: 10.1149/1.2220995

Chen, L., Lin, C., Zuo, J., Song, L., and Huang, C. (2004). First spectroscopic observation of peroxocarbonate/ peroxodicarbonate in molten carbonate. *J. Phys. Chem. B* 108, 7553–7556. doi: 10.1021/jp035749l

Chen, L.-J., Cheng, X., Lin, C.-J., and Huang, C.-M. (2002). In-situ Raman spectroscopic studies on the oxide species in molten Li/K_2CO_3. *Electrochim. Acta* 47, 1475–1480. doi: 10.1016/s0013-4686(01)00872-6

Claes, P., Thirion, B., and Glibert, J. (1996). Solubility of CO_2 in the molten Na_2CO_3-K_2CO_3 (42 mol%) eutectic mixture at 800 ^oC. *Electrochim. Acta* 41, 141–146. doi: 10.1016/0013-4686(95)00278-m

Frisch, M. J. E. A., Trucks, G. W., Schlegel, H. B., Scuseria, G. E., Robb, M. A., Cheeseman, J. R., et al. (2009). *Gaussian 09, Revision d. 01*.Wallingford CT: Gaussian. Inc, 201.

Hehre, W. J. (2002). Ab initio molecular orbital theory. *Acc. Chem. Res.* 9, 399–406.

Itoh, T., Abe, K., Dokko, K., Mohamedi, M., Uchida, I., and Kasuya, A. (2004). In situ raman spectroelectrochemistry of oxygen species on gold electrodes in high temperature molten carbonate melts. *J. Electrochem. Soc.* 151:A2042.

Kawase, M. (2017). Durability and robustness of tubular molten carbonate fuel cells. *J. Power Sources* 371, 106–111. doi: 10.1016/j.jpowsour.2017.10.024

Mendoza, L., Baddour-Hadjean, R., Cassir, M., and Pereira-Ramos, J. P. (2004). Raman evidence of the formation of LT-$LiCoO_2$ thin layers on NiO in molten carbonate at 650 C. *Appl. Surf. Sci.* 225, 356–361. doi: 10.1016/j.apsusc.2003.10.026

Morita, H., Komoda, M., Mugikura, Y., Izaki, Y., Watanabe, T., Masuda, Y., et al. (2002). Performance analysis of molten carbonate fuel cell using a Li/Na electrolyte. *J. Power Sources* 112, 509–518. doi: 10.1016/s0378-7753(02)00468-8

O'Boyle, N. M., Tenderholt, A. L., and Langner, K. M. (2008). cclib: a library for package-independent computational chemistry algorithms. *J. Comput. Chem.* 29, 839–845. doi: 10.1002/jcc.20823

Rosen, J., Geary, T., Hilmi, A., Blanco-Gutierrez, R., Yuh, C.-Y., Pereira, C. S., et al. (2020). Molten carbonate fuel cell performance for CO_2 capture from natural gas combined cycle flue gas. *J. Electrochem. Soc.* 167:064505. doi: 10.1149/1945-7111/ab7a9f

Scaccia, S., and Frangini, S. (2009). Effect of Ba and Ca additions on the oxygen solubility properties of a (70/30) mol% Li_2CO_3/Na_2CO_3 carbonate melt. *J. Mol. Liq.* 146, 39–43. doi: 10.1016/j.molliq.2009.01.011

Tong, J., Lei, X., Fang, J., Han, M., and Huang, K. (2016). Remarkable O_2 permeation through a mixed conducting carbon capture membrane functionalized by atomic layer deposition. *J. Mater. Chem. A.* 4, 1828–1837. doi: 10.1039/c5ta10105k

Watanabe, T., Izaki, Y., Mugikura, Y., Morita, H., Yoshikawa, M., Kawase, M., et al. (2006). Applicability of molten carbonate fuel cells to various fuels. *J. Power Sources* 160, 868–871.

Zhang, L., Huang, X., Qin, C., Brinkman, K., Gong, Y., Wang, S., et al. (2013). First spectroscopic identification of pyrocarbonate for high CO_2 flux membranes containing highly interconnected three dimensional ionic channels. *Phys. Chem. Chem. Phys.* 15, 13147–13152. doi: 10.1039/c3cp52362d

Zhang, L., Tong, J., Gong, Y., Han, M., Wang, S., and Huang, K. (2014). Fast electrochemical CO_2 transport through a dense metal-carbonate membrane: a new mechanistic insight. *J. Membr. Sci.* 468, 373–379. doi: 10.1016/j.memsci.2014.06.028

Zhang, P., Tong, J., Jee, Y., and Huang, K. (2016). Stabilizing a high-temperature electrochemical silver-carbonate CO_2 capture membrane by atomic layer deposition of a ZrO_2 overcoat. *Chem. Commun.* 52, 9817–9820. doi: 10.1039/c6cc04501d

Conflict of Interest: The authors declare that the research was conducted in the absence of any commercial or financial relationships that could be construed as a potential conflict of interest.